COMPARISON OF THE CORROSION PROPERTIES OF CoCrMo DENTAL ALLOYS IN ARTIFICIAL SALIVA

PRIMERJAVA KOROZIJSKIH LASTNOSTI CoCrMo DENTALNIH ZLITIN V UMETNI SLINI

Tadeja Kosec[1], Mirjam Bajt Leban[1], Matej Kurnik[2], Igor Kopač[2*]

[1]Slovenian National Building and Civil Engineering Institute, Dimičeva ulica 12, Ljubljana, Slovenia
[2]Medical Faculty, University of Ljubljana, Vrazov trg 22, Ljubljana, Slovenia

CoCrMo alloys are known for their biocompatible properties, which, together with their favorable mechanical properties, mean they can be efficiently used in dentistry. With the development of selective laser melting for the fabrication of 3D-printed objects, interest in the corrosion properties of this alloy has risen in the field of prosthodontics. In the study, CoCrMoW dental alloys were studied in artificial saliva at body temperature, i.e., 37 °C. Different forms of CoCrMoW alloy were selected: a reference sample, i.e., original material as received from the supplier, a cast sample acquired from an ordinary procedure in a dental laboratory, and two 3D-printed samples made from CoCrMoW powder using the selective laser melting (SLM) method. Electrochemical, spectroscopic and hardness measurements were conducted. It was shown that the reference and cast samples have similar microstructural and electrochemical properties, while the electrochemical properties of the 3D-printed samples differ, most probably due to the effect of the higher micro porosity and chemical composition of the alloys.

Keywords: CoCrMo dental alloys, artificial saliva, additive technology, precision casting, corrosion

CoCrMo-zlitine so znane po svojih biokompatibilnih lastnostih, ki jih zaradi ugodnih mehanskih lastnosti vse pogosteje uporabljamo v zobozdravstvu. Z razvojem selektivnega laserskega taljenja (SLT) se je zanimanje za izdelavo 3D tiskanih predmetov in preučevanje korozijskih lastnosti teh zlitin povečalo tudi v stomatološki protetiki. V študiji je bila preučevana CoCrMoW-zlitina v umetni slini pri telesni temperaturi 37 °C. Izbrane so bile različne oblike zlitin CoCrMoW: originalni referenčni vzorec dostavljen od dobavitelja, kovinski ulitek, pridobljen z ustaljenim postopkom v zobotehničnem laboratoriju in dva 3D vzorca iz prahu CoCrMoW, ki sta bila izdelana z uporabo metode selektivnega laserskega taljenja. Izvedene so bile elektrokemijske in metalografske preiskave z merjenjem trdote. Ugotovljeno je bilo, da imata referenčni in ulit material podobne mikrostrukturne in elektrokemijske lastnosti, medtem ko imajo vzorci 3D tiska različne elektrokemijske lastnosti, najverjetneje zaradi učinka večje mikro poroznosti in kemijske sestave zlitin.

Ključne besede: CoCrMo dentalne zlitine, umetna slina, aditivne tehnologije, precizilsko ulivanje, korozija

1 INTRODUCTION

CoCrMo alloys are known for their biocompatible properties. They are resistant to wear and corrosion and possess high values of hardness and compressive strength.[1,2] Their use in orthopedics dates to the 1930s,[3] while their use in dentistry has increased over the last decade, due to the use of CoCrMo powder for the production of different dental assets through methods of novel additive technology, namely, selective laser melting (SLM).[4–8]

CoCrMo alloys as a biomedical alloy have been extensively studied, especially regarding their characteristics of corrosion.[4–13] Different physiological solutions have been used as corrosion media, including Hank's solution, phosphate physiological solution, PBS, saline solution (0.9 % NaCl), Minimum Essential Media (MEM), and artificial saliva. The effect of complexing agents and proteins, such as Bovine serum or albumin, has also been thoroughly reported.[11,12] Artificial saliva is the proper medium for corrosion studies investigating the corrosion of CoCrMo alloys for use in dental applications. Artificial saliva consisting of different chlorides, phosphates, carbonates, tianocyanates and citric acid was chosen for the present study.[14]

CoCrMo alloys spontaneously oxidize in air. The composition of the passive film is similar whether it is formed in air or during potentiodynamic polarization. The passive film consists of CrO_3 and/ or $Cr(OH)_3$. During a potentiodynamic scan, Co and Mo enter the passive film at potentials more positive than 0.3 V, as was studied with X-ray photoelectron spectroscopy at different potentials in the anodic region. Co is present as CoO and Mo as MoO_3, with an increase in the thickness also reported at anodic potentials of 0.4 V and 0.7 V.[13]

A transpassive peak in the anodic region of the potentiodynamic curve is sometimes observed; this is due to the formation of Cr(VI) species, which is found in oxide films formed in solutions containing phosphate.[10,11]

The electrochemical/corrosion properties of CoCrMo dental alloys are defined in our research. In order to study the differences in corrosion and mechanical prop-

*Corresponding author's e-mail:
igor.kopac@mf.uni-lj.si (Igor Kopač)

erties, different forms of the alloy were studied, namely a reference sample (an original metal disc received from the supplier, as incoming materials), a cast sample and 3D-printed samples made using CoCrMo powder as the source material. The second goal of the study was to define the differences in SLM printing parameters: the first sample was printed with optimal parameters and the second one with non-optimal parameters, which led to higher porosities.

The microstructural, physical and corrosion properties of the different forms of CoCrMo alloys are defined and compared. The effects of the microstructure, porosity, and hardness were sought in relation to the properties of corrosion and performance.

2 MATERIAL AND METHODS

Electrochemical tests were conducted using a Gamry ref 600 + Potentiostat/Galvanostat (USA, 2015). First, the open-circuit potential (OCP) was measured for at least 2 h, or until a steady state was achieved. Linear polarization measurements followed, using a scan rate of 0.1 mV/s in the potential range ± 20 mV vs E_{corr} (results not shown in this study). Electrochemical impedance spectroscopy measurements were then taken by measuring the impedance at different frequencies between 65 kHz and 1 mHz, using a perturbation signal of 20 mV and measuring 7 points per decade. Finally, potentiodynamic measurements were executed starting at –250 mV cathodically vs E_{corr}, progressing in the anodic direction up to 1.2 V or 1 mA/cm^2 at a scan rate of 1 mV/s. Different electrochemical parameters were extracted from the electrochemical measurements using Echem Analyst Software.

The corrosion cell for the electrochemical tests consisted of an assembly of three electrodes in a jacked cell with a volume of a 350 cm^3, using an Ag/AgCl reference electrode and a graphite rod as a counter electrode. The areas of the working electrodes were as follows: 3D-printed samples 0.64 cm^2, the reference sample 0.278 cm^2, and the cast sample 0.65 cm^2. All the results

presented were normalized. The working electrodes and the electrochemical cell for the corrosion testing are presented in **Figure 1**.

The electrolyte for the corrosion studies was simulated saliva, containing 0.6 g/L NaCl, 0.72 g/L KCl, 0.22 g/L CaCl$_2$·2 H$_2$O, 0.68 g/L KH$_2$PO$_4$, 0.856 g/L Na$_2$HPO$_4$·12 H$_2$O, 0.060 g/L KSCN, 1.5 g/L KHCO$_3$ and 0.03 g/L citric acid and having a pH of 6.5.[14] All measurements were conducted at body temperature, i.e., 37 °C, using an external heating unit that sustained a constant temperature.

All specimens were prepared using wet abrasion with up to 1200-grit SiC emery paper and ultrasonically cleaned in acetone for 3 min.

CoCrMoW was supplied in powder form by Scheftner, and had a composition in mass fraction as follows: 61 *w*/% Co, 27.5 *w*/% Cr, 8.5 *w*/% W, 3.5 *w*/% Mo, 1.6 *w*/% Si, C, Fe and Mn ≤ 1 *w*/%. The reference sample, a disc supplied by Scheftner, had the same chemical composition. For the cast sample the composition was as follows: 63.3 *w*/% Co, 24.8 *w*/% Cr, 5.3 *w*/% W, 5.1 *w*/% Mo and 1 % Si, Ce < 1 *w*/%.

The SLM samples were printed at two different energy densities – low (78.1 J/mm^3) and high (153.8 J/mm^3) – in order to study the difference between the optimal and non-optimal printing parameters chosen. The latter resulted in a porous structure, while the former resulted in the samples having minimal porosity.

Light microscopy on the metallographically prepared samples at different magnifications was executed using a Carl Zeiss metallographic microscope (Germany, 2009).

3 RESULTS AND DISCUSSION

3.1 Microstructure, porosity and hardness

First, the samples were metallographically prepared (**Figure 2**) and investigated using light microscopy at different magnifications. The porosity of each sample was defined at 12.5-times magnification with image analysis using ImageJ software according to the standard
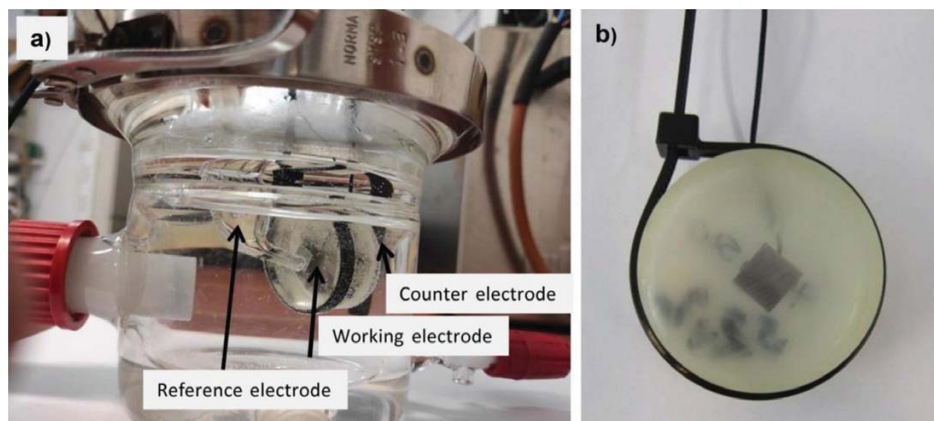

Figure 1: Photographic images: a) electrochemical cell, b) working electrode, fabricated for 3D-printed cube in epoxy resin with an electrical contact
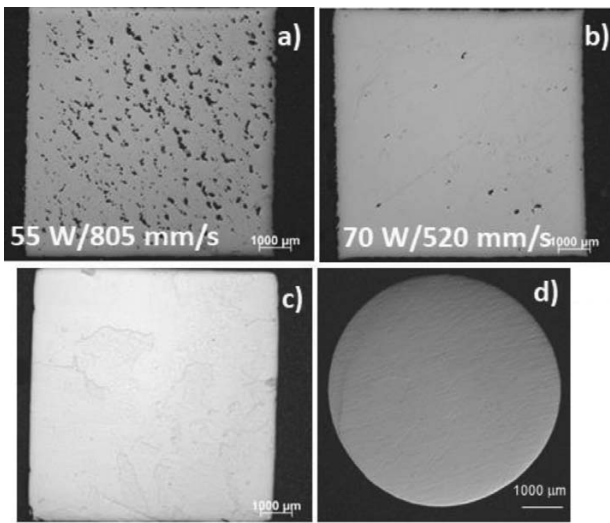
Figure 2: Photographic images of samples observed by optical microscopy at 12.5× magnification to observe the porosity and microstructure

ASTM E2109-01.[15] Hardness measurements were then executed with a minimum of 6 measurements taken for each sample. The results are presented in **Table 1**.

Table 1: Vickers hardness HV and porosity values

sample	E/(J/mm^3)	Porosity (%)	HV 0.3	HV 10
CoCrMo 55 805	78.1	4.8	417 ± 28	356 ± 21
CoCrMo 70 520	153.8	0.1	409 ± 27	390 ± 5.3
CoCrMo ref	/	0	361 ± 19	302 ± 9.4
CoCrMo cast	/	0	312 ± 13	305 ± 6.3

It can be observed that the CoCrMo samples printed at a low energy density (78.1 J/mm^3) were highly porous (4.8 %), while the sample printed with optimal laser parameters had an acceptable porosity as low as 0.1 %. Porosity also had a significant impact on the mechanical properties – namely, the higher porosity, the lower the hardness of the material. From the hardness measurements in **Table 1** the printed specimens exhibited a higher hardness compared to the reference and cast samples. The main reason for this is the finer microstructure, cellular dendrites and elongated participates, which acted as obstacles to dislocation movement.[16–18] By comparing the printed specimens it can be seen that there is no significant difference between the specimens printed with low and optimal parameters when a low load is used for the hardness measurements (HV 0.3, 2.93 N). On the other hand, hardness measurements performed at a higher load (HV 10, 98 N) showed that the highly porous specimen had lower hardness, as a greater average surface area was considered, which is a more representative property than HV 0.3.

Comparing the hardness of the reference and cast samples, the HV 10 hardness is similar, whereas the HV 0.3 hardness is significantly higher in the reference material. The reference material is also cast, but it is very possible that it contained a larger amount of Mo than the cast specimen after casting in the dental shop. Casting in a dental laboratory is performed in atmospheric conditions, and not in a vacuum or protective atmosphere. Due to this, Mo, which (besides W and C), contributes the most to the final hardness, also forms MoO_3, which easily evaporates above 450–500 °C. The vapour pressure of the MoO_3 becomes significant, and at higher temperatures, depending on the total partial pressure of oxygen, the rate of evaporation of the MoO_3 equals its rate of formation.[19,20] An additional EDS analysis was performed on the samples in order to compare the amount of Mo and W in the samples. It was found that the reference, cast, and 3D samples contained similar amounts of Mo (1.88–2.39 w/%), while the amount of W was 2.76–3.38 w/% in the cast sample and 5.69–5.94 w/% in the 3D-printed samples.

If we compare the microstructure of the reference sample with the sample cast from the reference material at a higher magnification (100×) we can observe a finer dendritic microstructure in the reference materials, which should lead to a higher hardness,[17] as was stated earlier in this article.
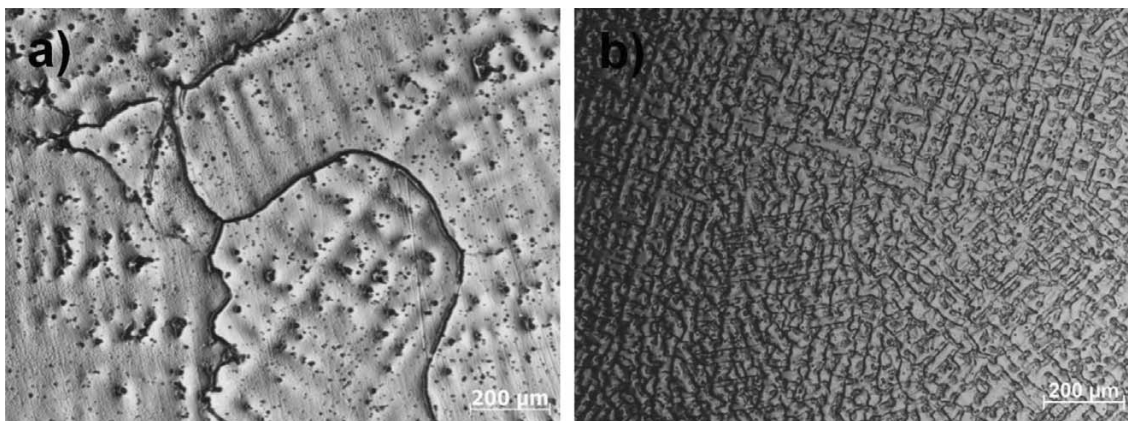

Figure 3: Microstructure of Co-Cr alloy, magnification 100×, electrolytically etched (100 mL H_2O + 4 mL HCl, 5 V, 10 s): a) reference sample, b) cast sample

3.2 Open-circuit potential measurements

The corrosion studies included a measurement of the open-circuit potential, linear polarization measurement, electrochemical impedance spectroscopy and potentio-dynamic measurements. The results of the linear polarization measurements are not presented in this study. When CoCrMo samples were immersed in artificial saliva at 37 °C, the potential slowly started to increase (**Figure 4**). The increase in potential upon exposure to the saliva indicates the growth of a passive layer. The potential of the reference sample of CoCrMo was –0.399 V at 2 h of immersion. The potential of the cast sample was slightly more positive, at –0.391 V. The most positive OCP potential of the SLM fabricated CoCrMo alloys, at –0.223 V, occurred in the sample printed at 55 W and 805 mm/s. The samples with a higher power (70 mm/s and 520 mm/s) and slower scanning speed had a slightly more negative potential (–0.244 V) after 2 h of exposure to artificial saliva at 37 °C.

3.3 EIS

Electrochemical impedance measurements were taken once a steady state was reached. It can be observed that the impedance responses for the reference, cast and 3D-printed samples are different (**Figure 5**). The highest impedance response was measured on the reference sample and the 3D-printed sample with a lower power and high scan rate (P = 55 W, laser scan speed 805 mm/s) and the highest measured porosity. The absolute impedance of these two samples at the lowest measured frequency was very high, with values of 1.42 MΩ·cm^2 and 2.37 MΩ·cm^2, respectively. The high value for the 3D printed sample might be due to its high porosity, meaning it has a higher specific area and high impedance due to the formation of a passive layer at places where an oxide layer had not formed, and the presence of a thick ox-
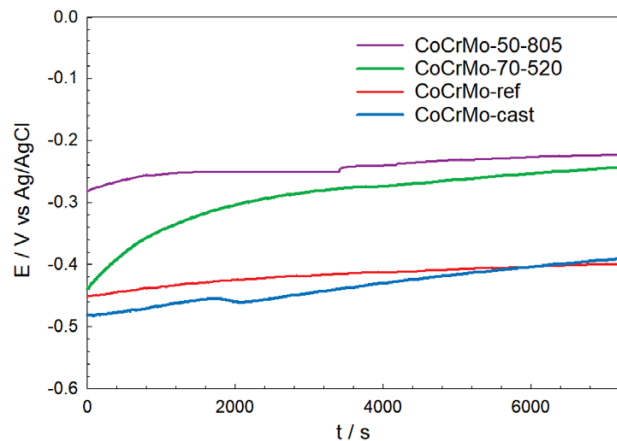

Figure 4: Evolution of E_{corr} for the CoCrMo samples (SLM method, reference and cast sample) in artificial saliva at 37 °C

ide layer resulting from the oxidative porosity. It has previously been reported that higher polarization resistance values occur in samples which have a passive film in the anodic region,[11] as could be the case in the porous 3D-printed CoCrMo alloy sample. In contrast, the 3D-printed sample (P = 70 W, 520 mm/s) had the smallest absolute impedance at the lowest measured frequency (475 kΩ·cm^2).

The cast CoCrMo sample had an impedance response value of 653 kΩ·cm^2.

The SLM specimens contained a far higher concentration of W (9.5 w/%) than the cast specimens (5.1 w/%). The addition of W is known to improve the corrosion resistance of Co-Cr alloys.[21]

3.3 Potentiodynamic polarization measurement

Potentiodynamic curves for the cast sample, the reference material and the 3D-printed alloys are given in **Figure 6**. There are some important observations which
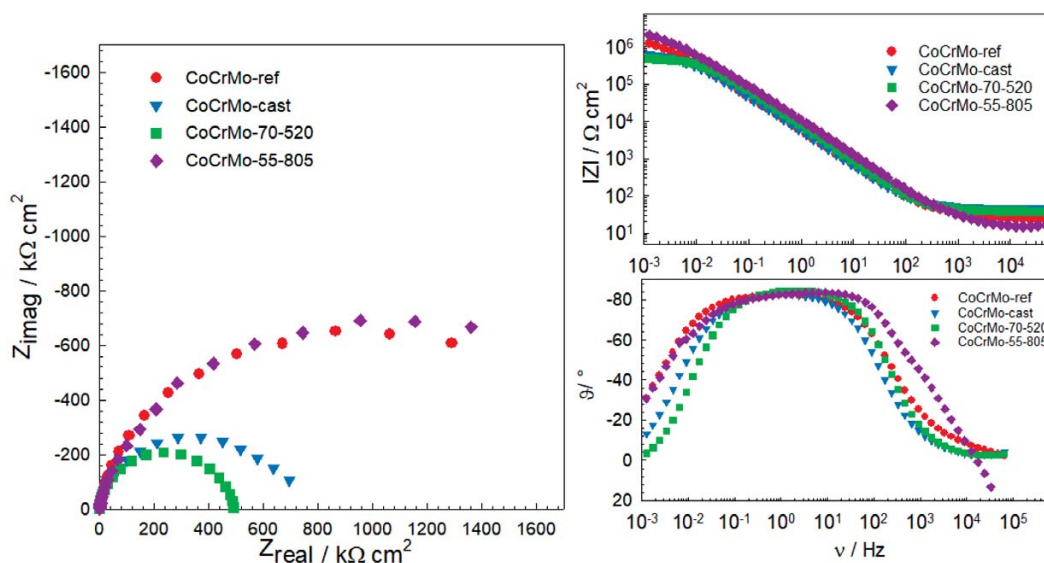

Figure 5: Nyquist and Bode plots of CoCrMo (ref., cast and SLM samples, printed with different parameters) in simulated saliva at 37 °C

Table 2: Corrosion potential, corrosion current and corrosion rate for all samples obtained from cyclic polarization

Sample	E_{OCP}/V	E_{corr}/V	j_{corr}/(nA cm^{-2})	E_b/V	ΔE (E_b–E_{corr})/V
CoCrMo SLM 55_805	−0.223	−0.265	13.6	0.436	0.701
CoCrMo SLM 70_520	−0.244	−0.217	22.1	0.417	0.634
CoCrMo Reference	−0.399	−0.533	16.9	0.749	1.28
CoCrMo Cast	−0.310	−0.391	21.5	0.742	1.13

allow differentiation between the various CoCrMo samples. Namely, the corrosion potential, E_{corr}, is more positive in the SLM fabricated samples, and they have similar values. The corrosion potentials of the reference and cast samples, however, were more negative, with the reference sample having the lowest value, at −0.533 V (**Table 2**). The values of the corrosion current density, j_{corr}, are similar for all the samples, with values between 13.6–22.1 nA/cm².

There is a slight difference in the behavior of the various CoCrMo samples in the anodic region of the potentiodynamic curve. Lower anodic current densities were observed in the 3D-printed samples in a "pseudo passive region" of the potentiodynamic curve. Since E_{corr} was more positive, the potential range where the current density is constant, is narrower in comparison to the cast and reference samples (ΔE in **Table 2**). The more positive corrosion potential and narrower passive region might be related to the increased effective surface resulting from the open porosities of the SLM-fabricated samples. The reference sample and the SLM-fabricated sample (55 W, 805 mm/s) exhibited transpassive behavior with a decrease in current in the transpassive region, which is related to the increased action of Cr (VI) in the passive film.[13]

3.4 Optical microscopy

Following the potentiodynamic (PD) scans, the surfaces exposed to artificial saliva were inspected. As observed from the images after the PD scans, defects in the form of spots can be observed. These are not pits but rather the state of the surface after the experiments, where the surface change is observed at the sites of the pores in the form of round spots. These are circled in **Figure 7**.

The 3D-printed sample with a higher porosity (50 W, 805 mm/s) showed a larger number of spots with a discoloured surface, as indicated by the black circles in **Figure 7f**. A similar, but less frequent, change in colour and texture appeared in the SLM fabricated sample printed at 70 W and 520 mm/s (**Figure 7b**). No indication of a modified surface was found on the cast sample (**Figure 7e**), while the reference sample had a small, elongated spot in the middle of the sample, although this did not affect its electrochemical properties (**Figure 7h**).
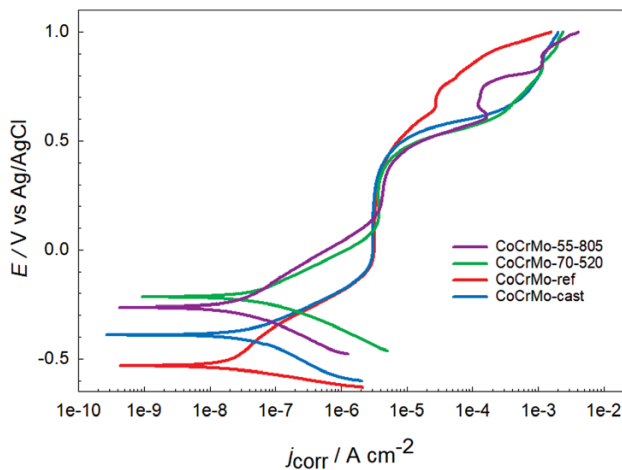
Figure 6: Potentiodynamic curves for the SLM fabricated samples and the cast and reference samples made from CoCrMo alloys in artificial saliva at 37 °C
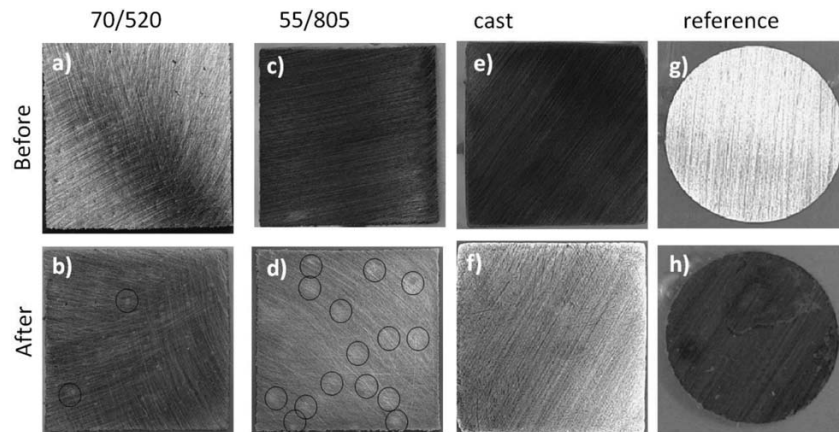
Figure 7: Optical microscopy and SEM examination of the type and extent of corrosion damage on the samples following the potentiodynamic experiments

4 CONCLUSIONS

This research investigated CoCrMoW dental alloys in artificial saliva at body temperature i.e., 37 °C. Different forms of CoCrMoW alloy were studied, i.e., a reference sample (material as received from the supplier), a cast sample (using an ordinary procedure in a dental cast shop), and two samples made from CoCrMoW powder using the selective laser melting method.

Microstructural, physical and corrosion studies showed that:

1. SLM-printed samples had a higher porosity than the reference and cast samples, with the high porosity being related to the printing parameters. The higher energy density obtained using optimal printing parameters resulted in a lower micro-porosity.

2. After 2 h of immersion in artificial saliva the corrosion potential was more positive in the SLM-printed CoCrMoW samples, due to the presence of oxides in open pores at the surface, while the corrosion potential of the reference and cast samples was more negative.

3. Electrochemical impedance spectroscopy measurements and potentiodynamic measurements showed similar electrochemical properties; the reference and cast samples had very similar properties while the SLM fabricated sample had diverse properties due to different levels of porosity.

4. The SLM specimens exhibited higher hardness than the reference and cast samples, which is due to the finer microstructure of the SLM specimens, and the presence of cellular dendrites and elongated participates, which acted as dislocation movement obstacles.

5. Due to the characteristics of the printed samples found it can be concluded that metal frameworks fabricated by SLM technology in clinical practice are suitable for long span bridges in fixed prosthodontics.

Acknowledgments

5 REFERENCES

[1] P. A. Schweitzer, Fundamentals of metallic corrosion: Atmospheric and Media Corrosion of Metals, Corrosion Engineering Handbook, 2nd ed., CRC press, Taylor&Francis Group, NY 2007

[2] H. V. Cruz, J. C. M. Souza, M. Henriques, L. A. Rocha, Tribocorrosion and BioTribocorrosion in the Oral Environment: The Case of Dental Implants, In: Biomedical Tribology, Ed: J. Paulo Davim, Nova Science Publisher, 2011

[3] D. McMinn, Birmingham Hip Resurfacing (BHR) history, development and clinical results, Midland Medical Technologies, Birmingham, U. K., 2000

[4] B. Konieczny, A. Szczesio-Wlodarczyk, J. Sokolowski, K. Bociong, Challenges of Co-Cr Alloy Additive Manufacturing Methods in Dentistry-The Current State of Knowledge (Systematic Review), Materials, 13 (2020), 3524, doi:10.3390/ma13163524

[5] T. Dikova, Properties of Co-Cr Dental Alloys Fabricated Using Additive Technologies, Biomaterials in Regenerative Medicine Chapter, (2018), 141–159, doi:10.5772/intechopen.69718

[6] C. dos Santos, A. F. Habibe, B. G. Simba, J. F. C. Lins, B. X Freitas, C.A. Nunes, CoCrMo-base Alloys for Dental Applications Obtained by Selective laser melting (SLM) and CAD/CAM, Mat. Res., 23 (2020), doi:10.1590/1980-5373-MR-2019-0599

[7] M. Zhang, Y. Yang, C. Song, Y. Bai, Z. Xiao, An investigation into the aging behavior of CoCrMo alloys fabricated by selective laser melting, J. Alloys Compounds, 750 (2018), 878–886, doi:10.1016/j.jallcom.2018.04.054

[8] Y. Lu, S. Wu, Y. Gan, J. Li, C. Zhao, D. Zhuo, J. Lin, Investigation on the microstructure, mechanical property and corrosion behavior of the selective laser melted CoCrW alloy for dental application, Materials Science and Engineering C, 49 (2015), 517–525, doi:10.1016/j.msec.2015.01.023

[9] F. Contu, B. Elsener, H. Bohni, Corrosion behaviour of CoCrMo implant alloy during fretting in bovine serum, Corrosion Sci., 47 (2005) 8, 1863–1875, doi:10.1016/j.corsci.2004.09.003

[10] A. W. E. Hodgson, S. Kurz, S. Virtanen, V. Fervel, C. A. Olsson, S. Mischler, Passive and transpassive behaviour of CoCrMo in simulated biological solutions, Electrochim. Acta., 49 (2004), 2167–2178, doi:10.1016/j.electacta.2003.12.043

[11] A. I. Munoz, S. Mischler, Interactive effects of albumin and phosphate ions on the corrosion of CoCrMo implant alloy, J. Electrochem. Soc., 154 (2007), 562–670, doi:10.1149/1.2764238

[12] C. Valero Vidal, A. I. Munoz, Electrochemical characterisation of biomedical alloys for surgical implants in simulated body fluids, Corros. Sci., 50 (2008), 1954–1961, doi:10.1016/j.corsci.2008.04.002

[13] I. Milošev, The effect of biomolecules on the behavior of CoCrMo alloy in various simulated physiological solutions, Electrochim. Acta., 78 (2012), 259–273, doi:10.1016/j.electacta.2012.05.1

[14] G. S. Duffo, E. Q. Castillo, Development of artificial saliva solution for studying the Corrosion Behavior of Dental Alloys, Corrosion., 60 (2004), 594–602, doi:10.1016/j.electacta.2012.05.1

[15] ASTM E2109-01 Test Methods For Determining Area Percentage Porosity In Thermal Sprayed Coatings, doi: 10.1520/E2109-01R14

[16] T. Puskar, D. Jevremovic, R. J. Williams, D. Eggbeer, D. Vukelic, I. Budak, A comparative analysis of the corrosive effect of artificial saliva of variable pH on DMLS and cast Co-Cr-Mo dental alloy, Materials, 6 (2014), 6486–6501, doi: 10.3390/ma7096486

[17] A. Takaichi, Suyalatu, T. Nakamoto, N. Joko, N. Nomura, Y. Tsutsumi, S. Migita, H. Doi, S. Kurosu, A. Chiba, N. Wakabayashi, Y. Igarashi, T. Hanawa, Microstructures and mechanical properties of Co-29Cr-6Mo alloy fabricated by selective laser melting process for dental applications, Journal of the Mechanical Behavior of Biomedical Materials, 21 (2013), 67–76, doi:10.1016/j.jmbbm.2013.01.021

[18] B. Vandenbroucke, J. P. Kruth, Selective laser melting of biocompatible metals for rapid manufacturing of medical parts, Rapid Prototyping Journal, 13 (2007) 4, 196–203, doi:10.1108/13552540710776142

[19] E. A. Gulbranson, K. F. Andrew, F. A. Brassart, The oxidation of molybdenum from 550 °C to 1700°C, Journal of the Electrochemical Society, 110 (1962), 952–959

[20] S. B. Lyon, 3.17 - Corrosion of Molybdenum and its Alloys, Editor(s): B. Cottis, M. Graham, R. Lindsay, S. Lyon, T. Richardson, D. Scantlebury, H. Stott, Shreir's Corrosion, Elsevier., (2010), 2157–2167, doi:10.1016/B978-044452787-5.00106-2

[21] S. H. Tuna, E. Karaca, İ. Aslan, G. Pekkan, N. Ö. Pekmez, Evaluation of corrosion resistance of Co-Cr alloys fabricated with different metal laser sintering systems, The journal of advanced prosthodontics, 12 (2020) 3, 114–123, doi:10.4047/jap.2020.12.3.114